MODELING OF BLOOD FLOW IN MICROVESSELS

Arezou Jafari, Piroz Zamankhan, S. Mohammad Mousavi, and Pertti Kolari

Laboratory of Computational Fluid & BioFluid Dynamics, Lappeenranta University of Technology, Lappeenranta, Finland

piroz@lut.fi

Abstract: In this paper several models are presented for microcirculation. A comprehensive continuum approach is proposed in which fluid structure interaction has been taken into account. Based on limitations imposed by computational resources, a more simplified model based on volume of fluid approach is suggested to simulate movements of RBCs from an arteriole to a venule via a capillary. The results show that no RBCs can enter the microvessels in the absence of chemical components such as nitric oxide (NO), which functions as a vasodilator. This observation supports the hypothesis suggested by Singel and Stamler (Nature, 2004, p. 297).

Introduction

Human blood is a suspension of cells with various shapes, deformabilities, and electric charge densities in a complex suspending medium (plasma). Hence, it may be anticipated that deformation and flow of blood should be similar to that of a suspension of deformable, aggregable particles [1].

The composition of the suspending cells such as erythocytes, leukocytes, and platelets can vary extensively. The suspending fluid (plasma) is usually a Newtonian [1] aqueous solution. However, the general rheological behavior of erythocytes (RBC) is a strong function of the rate of deformation. The cell interior is a concentrated solution of oxygen-binding protein hemoglobin which behaves as an incompressible fluid whose viscosity is higher than that of plasma [2].

The blood circulation involves flows through networks of tubes with diameters ranging from $1\,cm$ down to a few μm, driven by the pumping action of the heart [3]. The RBC-plasma suspension (blood) can be considered to be Newtonian at shear rates above $1000\ s^{-1}$. Note that high shear rate flows occur in channels with a characteristic diameter of $400\ \mu m$. In smaller channels, effects such as migration of RBCs transverse to the main flow could play a key role in flow dynamics. In fact, if aggregation does occur the secondary processes such as sedimentation and syneresis could become the rate-limiting mechanisms. In this light, a simple continuum model is not satisfactory for vessels with diameters well below $400\ \mu m$ such as microvessels [1].

The analysis of blood flow in microcirculation requires the combining of fluid dynamics and solid mechanics. Here, it is likely that cell-cell interactions as well as the effect of walls are controlling the blood flow dynamics. Note that microcirculation blood flow is precisely matched to metabolic requirements. In fact, hemoglobin molecules release the oxygen via microcirculation where due to low aqueous solubility of oxygen, it can diffuse through a short distance into oxygen-consuming tissues; typically of order $20-100\mu m$ [3].

It is known that microcirculation flow dynamics is significantly affected by arrangement, orientation and deformability of RBCs in plasma suspension [3]. The deformation of RBCs involves area dilation or condensation, surface shear, and bending or curvature changes [4]. The deformation of a cell membrane whose thickness could be as small as $5\,nm$ is modeled using a viscoelastic Kelvin model for which the viscous component represents the fluid-like behavior of the lipid bilayer, and the elastic component arises from the stretching of the cytoskeleton [5]. Note that the resistance to bending of cell membranes is relatively small [2]. However, bending moments become significant when the membrane curvature is large. In this case, the rheological behavior of erythocytes (RBC) should be a strong function of the rate of deformation.

Most of proposed models for blood flow in small vessels rely on two key simplifying assumptions. They are; the axisymmetric motion of red blood cells in capillaries, as well as the description of the flow of plasma between the cell and the wall using lubrication theory [3].

Recall that microcirculation blood flow is controlled by metabolic requirements. For example, a decrease in the oxygen content of blood (caused by increasing muscle activity) stimulates an increase in blood flow. On the other hand, blood flow decreases when the tissue oxygen consumption is reduced [6]. An important question remains concerning the hydrodynamic conditions at which RBCs from arterioles can enter microvessels in order to match to metabolic requirements. Indeed, the blood flow dynamics in branching has not been extensively explored.

Singel and Stamler [6] highlighted the role for the vasodilator nitric oxide (NO) in local modulation of the

ISSN: 1727-1983

diameter of small vessels in arterial blood flow. However, there is considerable debate over whether components such as NO could control blood traffic. This should open a new field of investigation including modeling of blood microcirculation, which requires considerations of the overall, NO biochemistry.

In this paper the question will be addressed of the effects of the flow dynamics in arterioles on RBCs approaching the microvessels.

The organization of the paper is as follows. In section II, a detailed overview is presented of modeling based on continuum type approach in blood flows useful for developing a simplified model for molecular dynamic type simulations of microcirculation. In section III, the developed model is applied to the specific example of flow in a branching where the blood is transferred from an arteriole to a venule via a capillary. Finally, the concluding remarks are presented in section IV, which may provide a correct methodology and a mathematical and numerical framework for the simulation of blood flows in microcirculation.

Continuum Type Approach

The nature of the blood flow within small vessels is important in determining its behavior, particularly since a key parameter in a suspension of deformable, aggregable particles such as blood is shear stress, which is determined by the flow field. In fact, cell biomechanics and blood flow include processes involving a broad range of length scales [3]. Note that the adhesion of a RBC to the wall of vessel as illustrated in Fig. 1 involves the deformation of the cell whose length is of the order of micrometer. However, the adhesion bonds between the RBC and wall could be on the order of the nanometers.

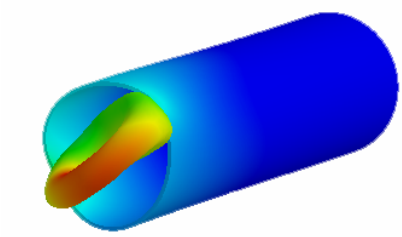

Figure 1: Interaction of an RBC and the wall of a capillary. The RBC is color coded by the local value of the effective stress magnitude.

In this light, the numerical modeling of microcirculation requires an accurate description of the cell adhesion by incorporating molecular and cellular information. In addition, any useful model of blood flow must account for the small vessels and the presence of cells and receptors in the capillary.

Indeed, the description of local phenomena such as cell adhesion and blood flow in microcirculation may be more accurately addressed by means of three-dimensional (3D) simulations, based on a multi-scale modeling approach. In these simulations the specification of boundary data is critical.

Note that cell adhesion involves receptors, cells, and vessels with a broad range of length scales from the order of nm and μm. The RBC membrane, which is a composite of the plasma membrane and the cytoskeletal network, is heterogeneous at the length scale of individual lipid molecules. Hence, it is of interest to use a discrete model for which space is divided into a lattice of points to describe the movement of a single cell. In fact, the models such as cellular large-Q Potts model [7] may be a useful technique for cell level simulation of tissues. This becomes more attractive if a continuous model can be developed to give rise to similar solutions as those obtained by the discrete model at length scales where their range of applicability overlap. This may provide insights into how discrete models can be used as a basis for the development of their continuous equivalents.

In the present study, the processes are considered on the scales longer than 100 nm where the membrane may be homogenous in its properties. Knowledge of the cell membrane mechanics including membrane elasticity and membrane shear viscosity may be obtained by analyzing a system, as shown in Fig. 2. Figure 2 illustrates cell membrane buckling and cell folding in numerical type experiments of micropipette aspiration which can be used to develop a reliable model for the red blood cell membrane.

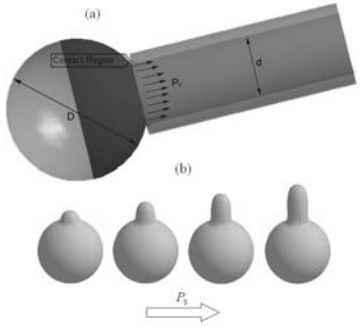

Figure 2: (a) The schematic of micropipette with some nomenclatures. Here, the vesicle diameter is $20\,\mu m$ and pipette caliber is $8\,\mu m$. (b) The variations of vesicle's shape with increasing suction pressure.

Recall that the problem of micropipette aspiration is concerned with the structures such as cell membranes with the thickness of 5 nm. The overall scale of the vesicle denoted by R_v, as illustrated in Fig. 3, is much larger than the thickness of the cell membrane. Many important features are involved, such as membrane-micropipette interactions, as well as membrane performance properties.

Using classical thin-shell theory the general equations of motion in referential coordinates for a

ISSN: 1727-1983

viscoelastic RBC membrane in absence of body forces may be given as [8].

$$\rho \ddot{u}_i = \tau_{ij,j}, \qquad (1)$$

The displacements in a global rectangular Cartesian coordinate system $X_j \left(j = 1,2,3 \right)$ are denoted by $u_i = x_i - X_i = u_i \left(X_j, t \right)$ with kinematical relations $\ddot{u}_i = \partial / \partial t^2 \, x_i \left(X_j, t \right)$. Equation (1) with constitutive equation for surface tension tensor $\tau_{ij} = \gamma \left(\delta_{ij} - n_i n_j \right) + \left(\mu_s' - \mu_s \right) \theta \left(\delta_{ij} - n_i n_j \right) + 2\mu_s E_{ij}$ and geometric equations $E_{ij} = 1/2 \left(\delta_{ik} - n_i n_k \right) \left(\delta_{jl} - n_j n_l \right) \left(u_{k,l} + u_{l,k} \right)$, provide equations for the unknowns comprising stresses σ_{ij}, six strains E_{ij}, and displacements u_i. Here, γ is the isotropic tension, θ is the rate of surface dilatation defined as $\theta = \left(\delta_{ij} - n_i n_j \right) u_{j,i}$, n is the unit normal vector for the interface, μ_s' and μ_s are two constants expressing the interface shear and dilatational viscosity.

The set of equations given above has to be solved for appropriate boundary and initial conditions listed below:

$$\begin{aligned} &\sigma_{ij} n_j = T_i \left(t \right), && \text{on } \partial b_1 \\ &\left(\sigma_{ij}\big|_{x_i^+} - \sigma_{ij}\big|_{x_i^-} \right) n_j = 0, && \text{on } \partial b_2 \\ &x_i \left(X_{j,0} \right) = X_i^0, \\ &\dot{x}_i \left(X_{j,0} \right) = V_i \left(X_j \right), \end{aligned} \qquad (2)$$

where T_i is traction loads vector.

The second condition in (2) represents the contact discontinuity given along an interior boundary ∂b_2 when $x_i^+ = x_i^-$.

The Galerkin formulation may be obtained from (1) and (2) by using the Gauss theorem. That is

$$\delta W = \int_{V_b} \rho \ddot{u}_i \delta u_i dV_b + \int_{V_b} \sigma_{ij} \delta u_{i,j} dV_b - \int_{\partial b_1} T_i \delta u_i dS_b = 0. \qquad (3)$$

This equation is the weak form of the equilibrium equations, and the load transfer occurs via boundary conditions (2). Note that no slip boundary condition is assumed for the fluid phase at the solid boundaries. Spatial discretization in numerical analyses such as binary collision of spheres could be typically based on a single method such as Lagrange, Euler, a mixture of Lagrange and Euler (Arbitrary Lagrange Euler), or meshfree Lagrangian (Smooth Particle Hydrodynamics). For the numerical simulation of the micropipette aspiration, each of the different solutions mentioned above has unique advantages and there is no single ideal numerical method which would be appropriate to the various regimes of a contact. The physical properties of micropipette are the elastic modulus, $E = 6.3 \times 10^{10}$ Pa, density, $\rho = 2500 \, kg/m^3$, and Poisson's ratio, $\nu = 0.244$.

In the present study, the Lagrange method of space discretization is used for which the numerical grid moves and deforms with the material.

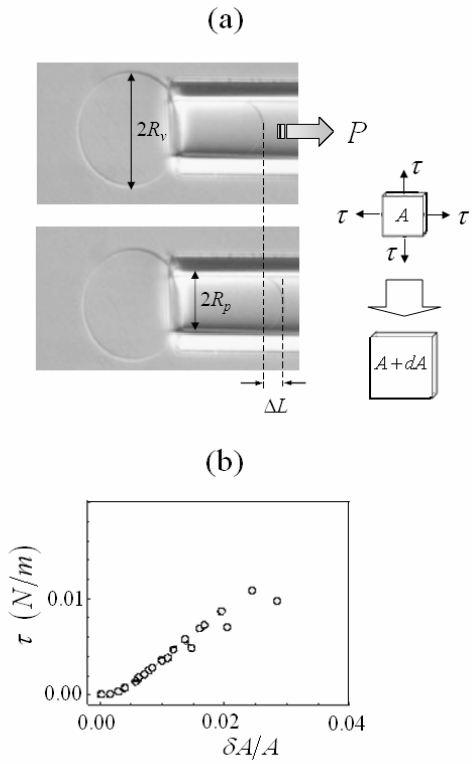

Figure 3: Schematic of vesicle pressurization and some nomenclature. (b) Numerical results of membrane tension and fractional area dilation for a system as shown in Figure 2.

Using the physical properties of a polymer membrane, the results for membrane tension as a function of fractional area dilation are obtained using the numerical method discussed earlier. Figure 3 (b) illustrates numerical results of membrane tension and fractional area dilation for a vesicle pressurized in a system as depicted in Fig. 2. Note that at high-tension regime, the slope of the tension versus area dilation approaches the direct elastic expansion modulus of the membrane. The results presented in Fig. 3 (a) are in qualitative agreement with those predicted using the simplified theory developed by Evans and Rawicz [9] for tension and bending elasticity in viscoelastic membranes.

The model capability is further assessed by predicting the deformation of an RBC interacting with the vessel wall at a branching of an arteriole and a capillary. As illustrated in Fig. 4, cell-wall interaction

ISSN: 1727-1983

could induce localized waves in the wall of the arteriole.

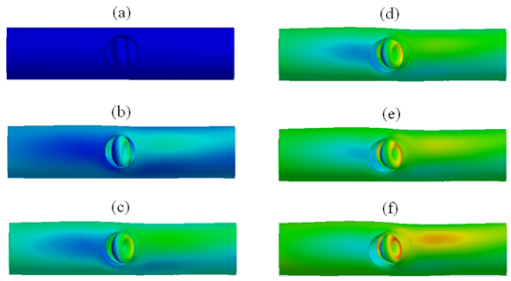

Figure 4: Temporal evolution of deformations in a branching. Note that a localized wave can easily be seen as a result of cell-wall interactions. Color represents the magnitude of tension, where red represents highest and blue shows the lowest. Here, no elastic behavior for the daughter is assumed whose diameter is $6.5\,\mu m$. The larger vessel diameter $13\,\mu m$, and the diameter of cell is $8\,\mu m$.

A continuum approach may be employed at the cellular level to account for moving boundaries. Figure 5(a) shows the mesh for a grid used for the simulation of RBC flows thorough a small vessel. In addition, Fig. 5 (b) represents more details of mesh for deformable RBCs whose deformation may be expressed by Eq. (1). The cell-cell interactions as illustrated in Figs. 5(c)-(d), denote the transfer of momentum due to collisions among the cells.

The numerical solution of incompressible Navier-Stokes equations accounting for moving boundaries, as illustrated in Fig. 5 (e), offers insights for a variety of problems including capillary fluid flow and adhesion dynamics. The Navier-Stokes equations are as follows:

$$V_{i,i} = 0$$
$$\rho V_{i,t} + \rho V_j V_{i,j} = -p_{,i} + \sigma_{ij,j} - \rho g \delta_{iy} \qquad (4)$$

where P is the static pressure , σ_{ij} is the stress tensor and ρg is the gravitational [13]. Here σ_{ij} is:

$$\sigma_{ij} = 2\mu S_{i,j}$$
$$S_{i,j} = \frac{1}{2}(V_{i,j} + V_{j,i}) \qquad (5)$$

where μ is the molecular viscosity.

Freely suspended RBCs have the form of biconcave disks, about $8\mu m$ in diameter and $2\mu m$ in thickness. As the shear rate increases, the shape of the red cells changes to an ellipsoid, and then to an elongated spindle-like shape with the long axis approximately aligned with the flow as illustrated in Fig. 5 (b). Note that a dynamic mesh is required to account for changes in flow domain according to deformation of RBCs. Because of the fluidity of the cell interior and the low resistance of the membrane to shear and bending deformation, RBCs can easily deform and squeeze through capillaries with diameter less than $8\mu m$. However the deformation is limited by the incompressibility of the interior fluid and strong resistance of the membrane to area changes.

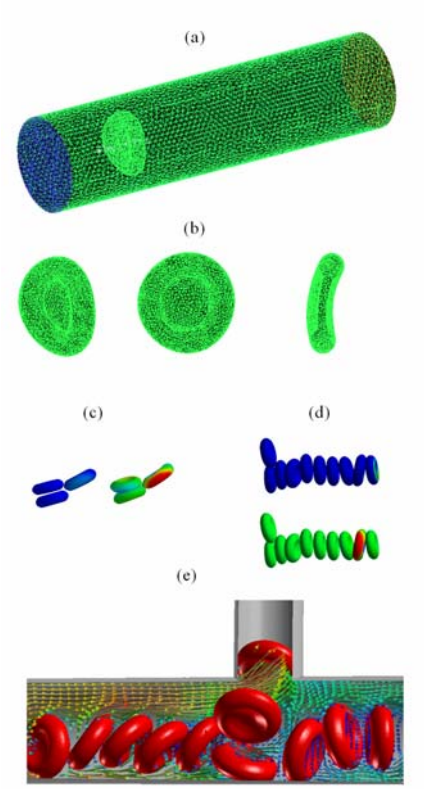

Figure 5: (a) The schematic of a suspended RBC in a capillary. Here, the vessel diameter and it's length are $50\,\mu m$ and $15\,\mu m$. (b) The deformation of RBC due to shear forces. (c-d) Mechanical interactions of red blood cells within the terminal vessels and at the branching site where the diameter of parent is $12\,\mu m$ and that of daughter is $6.5\,\mu m$ slightly smaller than the diameter of an RBC, which is $7.5\,\mu m$. (e) Velocity field of blood through the capillary.

The computed shapes are convex at the front and concave at the rear, in agreement with the experimental observation [10]. The predicted cell shape depends on the flow velocity [11]. As the velocity is increased, the cell contour becomes more streamlined. At high velocities, the full system of equations becomes increasingly difficult to be solved for a large number of RBCs. In this light, the important limitation of the scheme described in this section is that only a small number of moving particles can be studied using numerical methods.

Simplified Model

As mentioned earlier, the computational costs of the models discussed in the preceding section are high.

ISSN: 1727-1983

Hence, the single file motion of deformable RBCs in a branching where the blood moves from an arteriole to a venule via a capillary is simulated using volume of fluid (VOF) model [12]. Modeling of blood flow using VOF requires adding an extra term, F_i^{sv}, to equation (4) to account for the forces due to surface tension. That is, $\rho V_{i,t} + \rho V_j V_{i,j} = -p_{,i} + \sigma_{ij,j} - \rho g \delta_{iy} + F_i^{sv}$. In this case, there is no need of solid mechanic type computations as detailed in Sec. II using Eq. (1).

Note that a constitutive equation for the tensor of surface tension has been given earlier, namely $\tau_{ij} = \gamma\left(\delta_{ij} - n_i n_j\right) + \left(\mu_s' - \mu_s\right)\theta\left(\delta_{ij} - n_i n_j\right) + 2\mu_s E_{ij}$. It is straight forward to obtain an expression for the volume form of the surface tension force, F_i^{sv}, given by [14]

$$F_i^{sv} = \tau_{ij}\kappa\frac{F_{,j}}{[F]} \qquad (6)$$

where $[F]$ is the jump in the value of $F_{,j}$ across the interface and κ represents the curvature of the interface defined as

$$\kappa = \frac{1}{|F_{,i}|}\left(\frac{F_{,j}}{|F_{,i}|}\left|F_{,i}\right|_{,j} - F_{,ii}\right). \qquad (7)$$

Here the dynamics of blood is studied as a two-phase, non-homogeneous fluid consisting of liquid plasma and RBCs [13]. It is assumed that plasma is a uniform Newtonian- incompressible fluid with physical properties $\rho = 1000\,\mathrm{kg/m^3}$ and $\mu = 66\times10^{-3}\,\mathrm{kg/m.s}$ which flows in the gap between cells and vessel walls, and is described by the lubrication theory. So the fluid pressure is assumed to be uniform in the gap. The cells are composed of hemoglobin and randomly are entered the arteriole with physical properties of $\rho = 1000\,\mathrm{kg/m^3}$ and $\mu = 1.3\,\mathrm{kg/ms}$ [3].

The small arterioles and venules do not necessarily have all three tunics. The tunica media can be extremely reduced. This is shown in Fig. 6, in an arteriole. The tunica externa, in these conditions, is also extremely reduced or even absent.
So the tunica of arteriole and venule in the simplified model are not smooth.

Figure 6: Tunica of an arteriole [3]. Note the absence of smooth muscle cells in a capillary.

Figure 7 represents the geometry of the model. A regular grid throughout the domain is used, and the domain is discretized using 2×10^5 nodes and tetrahedral elements. The advantage of this approach is that the mesh does not evolve with time, reducing the computational expenses.

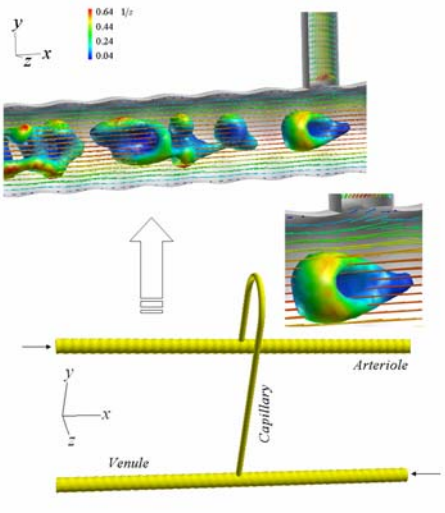

Figure 7: Geometry of simplified model and vectors plot of velocity field of blood through arteriole. Here the length of the vessels and RBCs sequently are 15μm and 8μm and the thickness of the RBCs is 2μm.

The constant pressure boundary conditions were assumed at the inlet and outlet of arteriole and venule. The inlet pressure for arteriole is set to 10 Pascal, whereas its outlet pressure is set to 10^{-3} Pascal. The values of inlet and outlet pressure of the venule are given as 5 Pascal and 10^{-3} Pascal, respectively. Hence, the RBCs are subjected to the pressure force, leading to their compression. These forces, which push RBCs to move toward the downstream, cause large deformations of RBCs as illustrated in Fig. 7. To obtain a better visualization, the RBCs in Fig. 7 are color coded with the local value of the strain rate. This may be of help in understanding the complex shapes of RBCs. Here, a strong vorticity can not be observed at the entrance of the capillary by which RBCs are to be directed into the capillary. In this light, a more generalized model would be required to investigate the importance of an appropriate kinetic/thermodynamic model for interaction of NO with hemoglobin to elucidate the detailed mechanism for oxygen delivery under physiological conditions [14].

In Fig. 8 an unreasonably high velocity is applied, which is two orders of magnitude higher than that used in the system as depicted in Fig. 7. The obtained results, as illustrated in Fig. 8, revealed that RBCs can be pushed into the capillary at high blood flow rates. However, it is quite unlikely that the condition as

ISSN: 1727-1983

presented in Fig. 8 could be present in a microcirculation of human beings. This observation supports the hypothesis that in low blood flow rate cases, similar to those found in human beings, a vasodilator such as NO would be required to cause RBCs to enter a capillary.

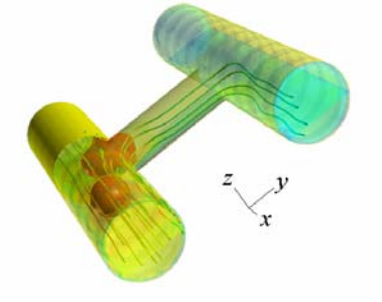

Figure 8: Shown are two RBCs in an arteriole, one of which entering a capillary perpendicular to the arteriole. In this case the inlet velocity of plasma is assumed to be 10 cm/s. The results imply that at unreasonably high plasma flow rates in a microcirculation a favorable vortex may be produced pulling the RBCs inside of the capillary.

An advantage of this model, and whose generalized version in which chemical reactions will be included, is that the role of anti-coagulant drugs can be investigated in irregular vessels, as illustrated in Fig. (9).

Figure 9: Aggregation and deformation of spherical RBCs in a irregular duct with length of 20μm .

Conclusion

Here several models were used to investigate deformation and flow of RBCs in microcirculation. Using a comprehensive model, it is shown that red cells never get stuck in capillaries, and negotiate these tiny vessels with ease. Using glass tiny capillaries, it has been shown that, down to about 3.5 microns diameter a red cell can be sucked into the tube without bursting the membrane.

Furthermore, a simplified continuum type approach is proposed. It has been shown that a model based on volume of fluid (VOF) can predict deformation and flow of RBCs in an arteriole successfully. It is well known that, with the exception of liver sinusoids, capillaries do not have muscle cells and are not subject to dilation through a nitric oxide mechanism. However, the results obtained highlight the importance of a vasodilator such as NO for controlling blood traffic in the microcirculation.

References

[1] SKALAK, R., AND CHIEN, S., (1987): 'Handbook of Bioengineering', McGraw-Hill Book Company.

[2] EVANS, E.A. (1983): 'Bending Elastic Modulus of Red Blood Cell Membrane Derived from Buckling Instability IN Micropipette Aspiration Tests', Biophys. J., 43, pp. 27-30.

[3] POZRIKIDIS, C. (2003): 'Modeling and Simulation of Capsules and Biological Cells', A CRC Press Company.

[4] EVANS, E., AND NEEDHAM, D. (1987): 'Physical Properties of Surfactant Bilayer Membranes: Thermal Transitions, Elasticity, Rigidity, Cohesion, and Colloidal Interactions', J. Phys. Chem., 91, pp. 4219-4228.

[5] EVANS, E.A., AND HOCHMUTH, R.M. (1976): 'Membrane viscoelasticity', Biophys.J. 16, pp. 1-11.

[6] SINGEL, D.J., AND STAMLER, J.S. (2005): 'Chemical Physiology of Blood Flow Regulation by Blood Cells: The Role of Nitric Oxide and S-Nitrosohemoglobin', Annu. Rev. Physiol, 67, pp. 99-145.

[7] TURNER, S., SHERRATT, J.A., AND PAINTER, K.J. (2004): 'From a Discrete to a Continuous Model of Biological cell Movement', Physical Review E 69, 021910.

[8] BILLINGTON, E.W., AND TATE, A. (1979): 'The Physics of Deformation and Flow', McGrow-Hill, International Book Company.

[9] EVANS, E., RAWICZ, W. (1990), Phys. Rev. Lett. 64, 2094.

[10] GAEHTGENS, P., DUHRSSEN, C., AND ALBRECHT, K.H. (1980): 'Motion, Deformation, and Interaction of Blood Cells and Plasma during Flow through Narrow Capillary Tubes', Blood Cells, 6, pp.799-812.

[11] SECOMB, T.W. (1987): 'Flow-Dependent Rheological Properties of Blood in a Capillaries', Microvasc. Res., 34, pp. 46-58.

[12] CHEN, L., GARIMELLA, S.V., REIZES, J.A., AND LEONARDI, E. (1999): 'The Development of a Bubble Rising in a Viscous Liquid', J. Fluid Mech. 387, pp. 61-96.

[13] BORYCZKO, K., DZWINEL, W., AND YUEN, D.A. (2003): 'Dynamical Clustering of Red Blood Cells in Cappilary Vessels', J Mol Model, 9, pp. 16-33.

[14] SINGEL, D.J., AND STAMLER, J.S. (2004): 'Red Blood Cell Vasodilation: Nitric Oxide and Haemoglobin Help to match blood flow to metabolic demand', P.297

.

ISSN: 1727-1983